Macromolecules

Article

pubs.acs.org/Macromolecules

Strictly Alternating Sequences When Copolymerizing Racemic and Chiral Acetylene Monomers with an Organo-Rhodium Catalyst

Yoshiaki Yoshida,[†] Yasuteru Mawatari,[*,†,‡] Takahiro Sasaki,[†] Toshifumi Hiraoki,[∥] Manfred Wagner,[⊥] Klaus Müllen,[⊥] and Masayoshi Tabata[*,§,#]

[†]Graduate School of Engineering, [‡]Research Center for Environmentally Friendly Materials, and [§]Center of Environmental Science and Disaster Mitigation for Advanced Research, Muroran Institute of Technology, 27-1 Mizumoto-cho, Muroran, Hokkaido 050-8585, Japan

[∥]Graduate School of Engineering, Department of Applied Physics, Hokkaido University, Sapporo, Hokkaido 060-8628, Japan

[⊥]Max Planck Institute for Polymer Research, Ackermannweg 10, D-55128 Mainz, Germany

[#]Faculty of Science and Technology, Department of Applied Chemistry and Bioscience, Chitose Institute of Science and Technology, Bibi 65-758, Chitose, Hokkaido 066-8655, Japan

Supporting Information

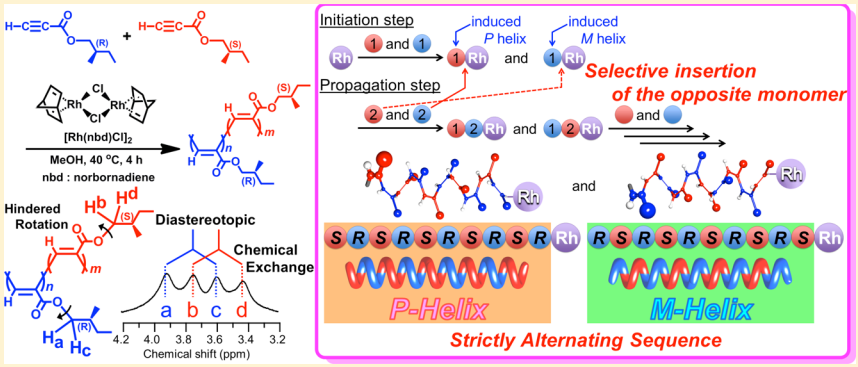

ABSTRACT: A racemic mixture and two chiral monomers of 2-methyl-1-butyl propiolate, i.e., ***rac*1**, ***R*1**, and ***S*1**, were stereoregularly polymerized with a catalyst, $[Rh(norbornadiene)Cl]_2$, in methanol at 40 °C to obtain the corresponding helical racemic and two chiral polymers, **P*rac*1**, **P*R*1**, and **P*S*1**, and a copolymer, **P*co***. The ^1H and ^{13}C NMR spectra of the racemic and chiral polymers differed, although the NMR spectra of their monomers were the same. The structures of the **P*co*** copolymers with different chiral monomer ratios were analyzed using 1D and 2D NMR, optical rotation, circular dichroism (CD), UV−vis, and computational methods to elucidate the stereochemical effect of the chiral monomers together with the polymerization mechanism. The temperature dependence of ^1H and ^{13}C NMR spectra in line shape and intensity indicated that the helical main chain undergoes restricted rotation around the ester methylene bonds $-O-CH_2-$ through a three-site jump exchange called an accordion-like helix oscillation (HELIOS). The energetically preferred structures of the helical-sense polymers **P*R*1** or **P*S*1** were simulated using the MMFF94 program. The dependence of the NMR spectral line shapes, optical rotations, and calculated structures on the monomer feed clearly indicated that the copolymers alternatively incorporate ***R*1** and ***S*1** to generate one-handed helical-sense chains. Based on these results, a polymerization mechanism is proposed, explaining a strictly alternating copolymerization that yields helical chains.

INTRODUCTION

Helical synthetic polymers, e.g., poly(alkyl methacrylate)s,[1] poly(isocyanide)s,[2] poly(isocyanate)s,[3] poly(silane)s,[4] and others,[5−10] have been prepared using various catalysts, e.g., (−)-(sparteine), $Ni(CN\text{-}t\text{-}C_4H_9)_4(ClO_4)_2$, $TiCl_3(OCH_2CF_3)$, or sodium in the presence of 15-crown-5.[1−10] Recently, an organo-rhodium complex catalyst, e.g., $[Rh(nbd)Cl]_2$ (nbd = norbornadiene), and alcohol or amine as a cocatalyst or solvent[11−14] were used to stereoregularly prepare helical-substituted polyacetylenes (HSPAs), e.g., poly(alkyl propiolate)s (PAPs),[15−17] poly(phenylacetylene)s (PPAs)[13,18−46] and its analogues,[21−37] and poly(naphthylacetylene).[47,48] PAPs are $(-HC{=}CCOOR-)_n$ with linear (R = $(CH_2)_6CH_3$) or branched (R = $CH(CH_3)(CH_2)_5CH_3$) alkyl chains, which were proven by ^1H and ^{13}C NMR spectroscopy in solution to possess a helical contracted *cis*−*cisoid* structure and stretched *cis*−*transoid* structure. Furthermore, these helical polymers exhibited a unique

Received: November 19, 2016
Revised: January 17, 2017

DOI: 10.1021/acs.macromol.6b02508
Macromolecules XXXX, XXX, XXX−XXX

accordion-like helix oscillation called a HELIOS mode in solution, although they possessed hexagonal or tetragonal packing in their solid phases.[15,49−54] The helical aromatic polyacetylenes (HAPAs) are remarkable polymers because they exhibit two different modes of π-conjugation, i.e., through bond conjugation within the helical main chains composed of approximately three helical monomer units and through space π-conjugation along the fairly long helical axis with approximately 3.4 Å as the π-stacking distance between side chains.[18−27,38−42,52−54] Therefore, the colors of the resulting HAPAs are quite different, e.g., pale yellow,[21−27] orange,[25,27] red,[21−27] violet,[24,26] and black,[21−27] and can be controlled by experimental conditions, such as temperature and solvent.[19,21−27] A helix inversion of SPAs with chiral or achiral side chains in solution has been proposed based on CD and UV−vis spectral data,[35,55−59] but further evidence to support this dynamic process is needed. Nevertheless, SPAs have proven valuable as advanced polymer materials, e.g., as a chiral stationary phase for optical resolution columns of racemic small molecules.[18−27,38−42] Detailed structural information on HSPAs is needed to rationalize the intrinsic functional properties. It is still not known whether the copolymers possess alternating, random, and/or block sequences, although knowledge of their microtacticity has been considered crucial for various types of vinyl or styrene polymers.[60−64] Using various pieces of spectroscopic evidence, we reveal strictly alternating monomer sequences in poly((*rac*)-2-methyl-1-butyl propiolate) (R = $CH_2CH(CH_3)CH_2CH_3$) composed of ***R*1** and ***S*1** monomer units in a ratio of 1:1. This structural information can be used to propose a prevailing polymerization mechanism.

EXPERIMENTAL SECTION

Measurements. Number- and weight-averaged molecular weights (M_n and M_w) of **P*rac*1**, **PR1**, and **PS1** were measured using a GPC 900-1 (JASCO, Tokyo, Japan) equipped with two Shodex K-806L columns and an RI detector. Chloroform was employed as an eluent at 40 °C, and poly(styrene) standards (M_n = 800−1 090 000) were used for calibration. ^{1}H NMR (500 MHz) spectra were measured on a JNM-ECA500 (JEOL, Tokyo, Japan) using chloroform-d_1 ($CDCl_3$) at 30 °C and *p*-xylene-d_{10} at 30, 80, 100, and 130 °C. ^{13}C NMR (125 MHz) spectra were also measured in $CDCl_3$ at 0, 30, 40, and 60 °C. Rotating frame Overhauser effect spectroscopy (ROESY) and nuclear Overhauser effect spectroscopy (NOESY) spectra were recorded on a JNM-ECA 920 (JEOL, Tokyo, Japan) spectrometer using $CDCl_3$ at 40 °C. All 2D NMR spectra were collected over 1024 complex points in *t*2 and into 256 points in *t*1 with a sweep width of 11.5 kHz at a mixing time of 100 ms. Optical rotation of monomers and polymers was measured on a P-1010 (JASCO, Tokyo, Japan) in $CHCl_3$ at room temperature. Enantiomer excess (ee) was calculated according to the literature.[65] Solution UV−vis and CD spectra of polymers were recorded on V570 and J-720WI (JASCO, Tokyo, Japan) spectrophotometers, respectively, in $CHCl_3$ at 30 °C. Energetically optimized dynamic conformations of polymers were simulated using a MMFF94 force field program (Wavefunction, Inc., Spartan '14 Windows version 1.1.0).[66] Spectral simulation of ^{1}H and ^{13}C NMR spectra was performed using a gNMR program.[67]

Synthesis of (*R*)-2-Methyl-1-butanol, 1b. (*R*)-2-Methyl-1-butanol (**1b**) was prepared using (*S*)-methyl 3-hydroxy-2-methylpropionate (**1b-1**) (Tokyo Chemical Industry) as a starting material in five steps according to the literature (Scheme 1a).[68] (*R*)-2-Methyl-1-butanol, **1b**: 66% yield, bp 85 °C/196 mmHg, $[\alpha]_D$ = +8.00 (*c* 1.00, $CHCl_3$). ^{1}H NMR ($CDCl_3$): δ 3.52, 3.43 (d, *J* = 10.5 Hz, 2H, OCH_2), 1.31 (br, 1H, −OH), 1.55 (oct, *J* = 6.7, 1H, $CH(CH_3)$), 1.45, 1.15 (m, 2H, CH_2CH_3), 0.92 (d, *J* = 6.7 Hz, 3H, $CH(CH_3)$), 0.91 (t, *J* = 7.4 Hz, 3H, CH_2CH_3). ^{13}C NMR (ppm): δ 67.8, 37.5, 25.9, 16.2, 11.4.

Scheme 1. Syntheses of (a) (*R*)-2-Methyl-1-butanol, 1b, (b) *rac*1, *R*1, *S*1, (c) P*rac*1, PR1, PS1, and (d) P*co* Using a Catalyst $[Rh(nbd)Cl]_2$ in MeOH for 4 h at 40 °C

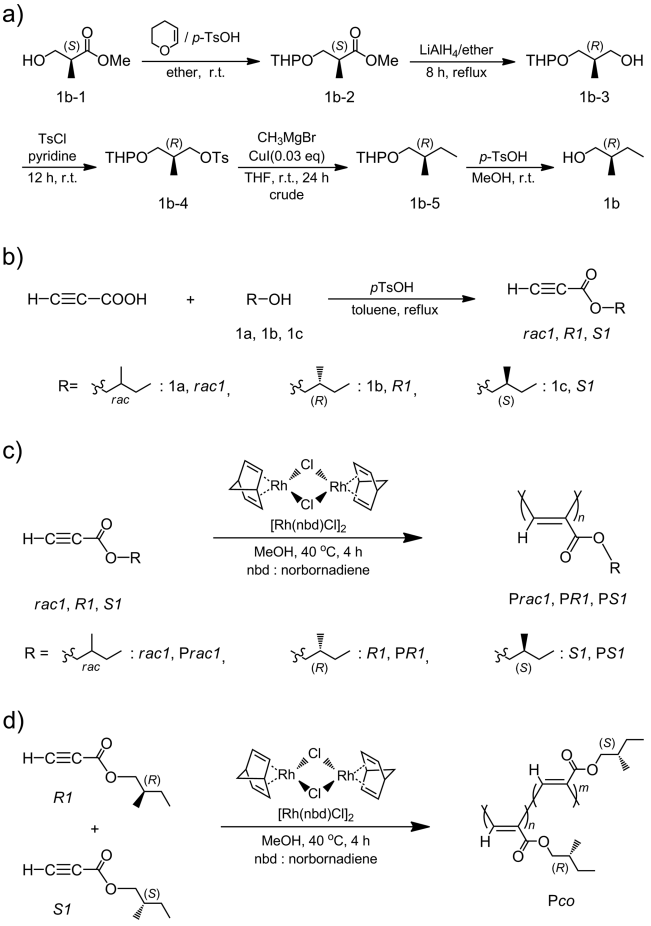

Synthesis of Monomers. DL-2-Methyl-1-butyl propiolate (***rac*1**), (*R*)-2-methyl-1-butyl propiolate (***R*1**), and (*S*)-2-methyl-1-butyl propiolate (***S*1**) were prepared from propiolic acid (Tokyo Chemical Industry) and the corresponding alcohol (**1a**, **1b**, **1c**) under acid catalysis according to the literature (Scheme 1a).[49−51] As a typical procedure, a mixture of 100 mL of toluene, 9.4 g (0.11 mol) of prepared **1b**, 11.9 g (0.17 mol) of propiolic acid (Aldrich), and 3.2 g (17 mmol) of *p*-toluenesulfonic acid monohydrate (Tokyo Chemical Industry) was refluxed for 8 h in a Dean−Stark apparatus. The resulting mixture was washed with saturated aqueous sodium hydrogen carbonate solution and distilled water. After the organic layer had been dried over anhydrous sodium sulfate, the solvent was removed by evaporation. The crude product was purified by distillation to give a colorless liquid ***R*1**, 7.7 g in 50% yield (Scheme 1b and Figure S1). ***rac*1**: 44% yield, bp 74 °C/24 mmHg. ^{1}H NMR (ppm): δ 4.09, 4.00 (d, *J* = 10.8 Hz, 2H, OCH_2), 2.88 (s, 1H, HC≡C), 1.77 (oct, *J* = 6.8 Hz, 1H, $CH(CH_3)$), 1.46, 1.22 (m, 2H, CH_2CH_3), 0.95 (d, *J* = 6.8 Hz, 3H, $CH(CH_3)$), 0.92 (t, *J* = 7.5 Hz, 3H, CH_2CH_3). ^{13}C NMR (ppm): δ 152.6, 74.4, 70.68, 33.9, 25.8, 16.2, 11.1. ***R*1**: 53% yield, $[\alpha]_D$ = −4.71 (*c* 1.00, $CHCl_3$). ***S*1**: 50% yield, $[\alpha]_D$ = +4.62 (*c* 1.00, $CHCl_3$).

Polymerization. Poly(DL-2-methyl-1-butyl propiolate) (**P*rac*1**), poly((*R*)-2-methyl-1-butyl propiolate) (**PR1**), and poly((*S*)-2-methyl-1-butyl propiolate) (**PS1**) were obtained by polymerization of the corresponding monomers, ***rac*1**, ***R*1**, and ***S*1**, using the $[Rh(nbd)Cl]_2$ catalyst as shown in Scheme 1c. In a typical procedure, 1.0 g (7.1 mmol) of the monomer and the calculated amount of the catalyst, 33 mg (7.1 × 10^{-2} mmol), were dissolved in MeOH (3.5 mL), and the mixture was stirred in a specially designed U-shaped ampule for 4 h at 40 °C.[11−14] The resulting reaction mixture was poured into excess

DOI: 10.1021/acs.macromol.6b02508
Macromolecules XXXX, XXX, XXX−XXX

methanol with stirring. The resulting pale yellow polymer was washed with methanol and dried under vacuum, ca. 10^{-2} Torr, for 12 h at room temperature. Copolymers composed of monomers of ***R*1** and ***S*1** were prepared using the calculated monomer ratio (mol %) of ***R*1** to ***S*1** according to the above method. The polymerization results are summarized in Table 2.

P*rac*1: ^{1}H NMR ($CDCl_3$): δ 6.81 (br, 1H, HC═C), 3.92, 3.75, 3.60, 3.43 (br, 2H, OCH_2), 1.68 (br, 1H, $CH(CH_3)$), 1.40, 1.16 (br 2H, CH_2CH_3), 0.89 (br, 3H, $CH(CH_3)$), 0.88 (br, 3H, CH_2CH_3). ^{13}C NMR (ppm): δ 163.9, 135.3, 128.0, 69.5, 33.8, 26.2, 16.56, 16.43, 11.20, 11.10. Anal. Calcd for $C_8H_{12}O_2$: C, 68.54; H, 8.63. Found: C, 68.74; H, 8.72.

PR1: ^{1}H NMR ($CDCl_3$): δ 6.81 (br, 1H, *HC*═C), 3.75, 3.60 (br, 2H, OCH_2), 1.67 (br, 1H, $CH(CH_3)$), 1.38, 1.15 (br 2H, CH_2CH_3), 0.88 (br, 3H, $CH(CH_3)$), 0.87 (br, 3H, CH_2CH_3). ^{13}C NMR (ppm): δ 163.9, 135.3, 128.0, 69.5, 33.8, 26.2, 16.5, 11.1. Anal. Calcd for $C_8H_{12}O_2$: C, 68.54; H, 8.63. Found: C, 68.72; H, 8.71.

PS1: ^{1}H NMR ($CDCl_3$): δ 6.81 (br, 1H, *HC*═C), 3.75, 3.60 (br, 2H, OCH_2), 1.67 (br, 1H, $CH(CH_3)$), 1.38, 1.15 (br 2H, CH_2CH_3), 0.88 (br, 3H, $CH(CH_3)$), 0.87 (br, 3H, CH_2CH_3). ^{13}C NMR (ppm): δ 163.9, 135.3, 128.0, 69.5, 33.8, 26.2, 16.5, 11.1. Anal. Calcd for $C_8H_{12}O_2$: C, 68.54; H, 8.63. Found: C, 68.73; H, 8.75.

RESULTS AND DISCUSSION

Polymerization. The polymerizations of three monomers, i.e., (***rac***)-, (***R***)-, and (***S***)-2-methyl-1-butyl propiolates, were performed using the catalyst $[Rh(nbd)Cl]_2$ at 40 °C for 4 h in MeOH to give the corresponding polymers, **P*rac*1**, **PR1**, and **PS1** as shown in Scheme 1c and Table 1. The polymers were produced in a moderate yield of 43−49%, a number-averaged molecular weight (M_n) of (2.1−3.2) × 10^4, and a molecular weight dispersity (M_w/M_n) of 4.9−5.5. The relative amounts of *cis* isomers (*cis* %) were determined to be 91−96% by comparing the relative intensities, i.e., $\underline{H}^{\alpha}$−C═C/C$\underline{H}_3$ of the main-chain vinyl proton at 6.80 ppm and the methyl proton at 0.87 ppm in the side chain of **P*rac*1**, **PR1**, and **PS1** (Figure 1 and Figure S2).[11−14] The optical rotations $[\alpha]_D$ of **PR1** and **PS1** were determined to be +813° and −847°, respectively, using chloroform at room temperature (Table 1). Copolymers, **P*co*s** were also prepared by changing the monomer ratio (mol %) of ***R*1** to ***S*1** using the $[Rh(nbd)Cl]_2$ catalyst at 40 °C for 4 h in MeOH, as shown in Scheme 1d and Table 2. The copolymers were also produced in a moderate yield of 41−44%, a number-averaged molecular weight (M_n) of (2.1−2.7) × 10^4, and a molecular weight dispersity (M_w/M_n) of 5.1−9.6,. The amount of *cis* configuration was determined to be 91−95% using the above-mentioned method. The $[\alpha]_D$ of copolymers is presented in Table 2. The resulting **P*rac*1**, **PR1**, **PS1**, and **P*co*** were soluble in $CHCl_3$ and toluene but insoluble in CH_2Cl_2, $C_2H_2Cl_4$, Et_2O, *n*-hexane, dimethyl sulfoxide, *N*,*N*-dimethylformamide, MeOH, and EtOH.

Table 1. Synthesis of P*rac*1, PR1, and PS1 Using $[Rh(nbd)Cl]_2$ in MeOH for 4 h at 40 °C[a]

polymer	yield[b] (%)	M_n[c] (×10^{-4})	M_w/M_n[c]	*cis*[d] (%)	$[\alpha]_D$[e]
P*rac*1	49	3.2	5.5	91	
PR1	43	2.1	4.9	96	+813
PS1	43	2.5	5.5	95	−847

[a]$[M]_0$ = 2.0 mol/L, $[M]_0/[cat.]$ = 100. [b]Insoluble fraction in methanol. [c]Estimated by GPC (PSt, $CHCl_3$). [d]Determined by ^{1}H NMR ($CDCl_3$). [e]*c* = 0.20 g/dL ($CHCl_3$).

^{1}H NMR Spectra of P*rac*1, PR1, and PS1. The ^{1}H NMR spectra of **P*rac*1**, **PR1**, and **PS1** were measured in $CDCl_3$ at 30 °C to deduce the helical structures that result from the highly stereoregular copolymerization induced by the Rh complex catalyst (Figure 1 and Figure S2). The important feature is that the ester methylene proton, i.e., O−C$H^{\varepsilon}H^{\varepsilon'}$, of the side chain was observed not as a singlet but rather as a four-peak signal at 3.92, 3.75, 3.60, and 3.43 ppm (Figure 1a). In contrast, the ^{1}H NMR spectra of **PR1** and **PS1** simply showed a two-peak signal at 3.75 and 3.60 ppm (Figure 1b and Figure S2), unlike the case of **P*rac*1**. The vinyl protons, H^{α}−C═, and all alkyl protons in the side chain were completely identical (Figure 1a and Figure S2).

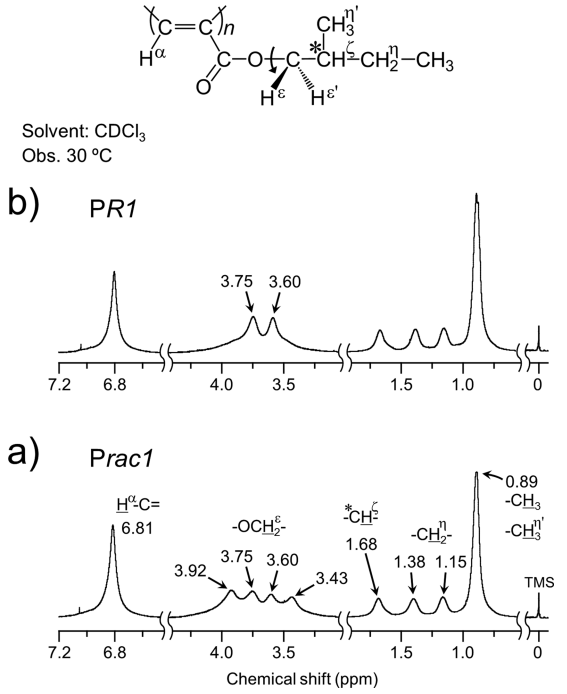

Figure 1. ^{1}H NMR spectra of (a) **P*rac*1** and (b) **PR1** prepared with $[Rh(nbd)Cl]_2$ in MeOH at 40 °C.

Table 2. Copolymerization Using *R*1 and *S*1 Monomers[a]

run	***R*1**:***S*1** (mol %)	yield[b] (%)	M_n[c] (×10^{-4})	M_w/M_n[c]	*cis*[d] (%)	$[\alpha]_D$[e]
1	10:90	43	2.1	8.5	91	−847
2	20:80	42	2.4	5.1	92	−779
3	30:70	41	2.5	9.5	92	−763
4	40:60	43	2.7	7.1	94	−636
5	50:50	41	2.6	6.6	93	0
6	60:40	44	2.4	9.6	93	+655
7	70:30	41	2.5	5.5	94	+781
8	80:20	44	2.7	5.1	95	+793
9	90:10	43	2.4	8.1	91	+806

[a]$[M]_0$ = 2.0 mol/L, $[M]_0/[cat.]$ = 100. [b]Insoluble fraction in methanol. [c]Estimated by GPC (PSt, $CHCl_3$). [d]Determined by ^{1}H NMR ($CDCl_3$). [e]*c* = 0.20 g/dL ($CHCl_3$).

Dependence of the Four-Peak Signal on Monomer-Feed Ratio As Detected by ^{1}H NMR. The copolymers **P*co*s** were prepared by mixing the chiral monomers ***R*1** and ***S*1** in the presence of the $[Rh(nbd)Cl]_2$−MeOH catalyst at 40 °C. The question is why the above four-peak signal is observed in the case of **P*rac*1**. Figure 2a shows the monomer-feed dependence of ^{1}H NMR spectra line shape for **P*co*** (Scheme 1d). The

DOI: 10.1021/acs.macromol.6b02508
Macromolecules XXXX, XXX, XXX−XXX

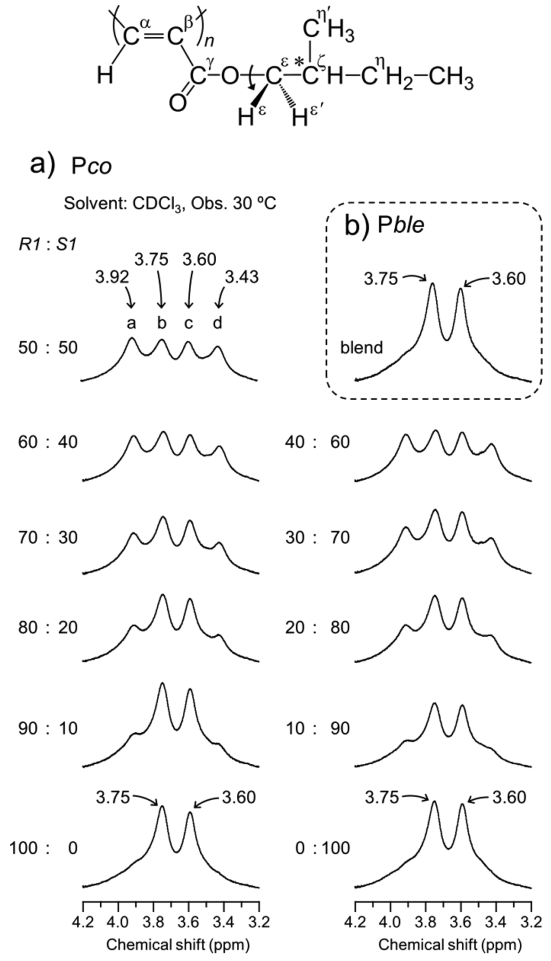

Figure 2. (a) Monomer-feed dependence of ^{1}H NMR spectra of **PR1**, **PS1**, and **Pco** and (b) ^{1}H NMR spectra of the blend polymer (**Pble**) observed at 30 °C in $CDCl_3$. **Pble** was obtained by mixing **PR1** with **PS1** at a molar ratio of 50:50 in $CDCl_3$.

intensities of the outer peaks indicate that **a** and **d**, at 3.92 and 3.43 ppm, respectively, decreased with increasing monomer ratio of either ***R*1** or ***S*1** within the copolymer. Inversely, the intensities of the inner two **b** and **c** peaks at 3.75 and 3.60 ppm gradually increased. However, the chemical shifts and the line shapes of the other alkyl side chain, and the vinyl protons, H^{α}–C= remained unchanged. The shapes of the four peaks of **Pco** agreed with that of **Prac1** when the monomer ratio of ***R*1** and ***S*1** was 50:50. A two-peak signal at 3.75 and 3.60 ppm observed in **PR1** or **PS1** was also observed for the blend polymer, **Pble** (Figure 2b), obtained when mixing **PR1** with **PS1** at a molar ratio of 50:50 in $CDCl_3$, although with this method the four-peak signal never appeared. This suggests that the main chains of copolymers **Prac1** and **Pco** are composed of a chiral monomer sequence different from that of chiral homopolymers as follows: neither a random nor a block monomer sequence, but rather *a strictly alternating monomer sequence* has been formed. Furthermore, the intensity changes in the four-line signal are attributed to the ratio of sequences in **Pco**s, i.e., sequences composed of only one monomer (identical to **PR1** or **PS1**) or an alternating monomer sequence (identical to **Prac1**).

Temperature Dependence of the Line Shapes of OCH^{ε}_2 Protons. The intensity of the two peaks observed at 3.75 and 3.60 ppm in **PR1** or **PS1** was not of equal intensity; instead, the intensity ratio reversibly changed to a fairly sharp and asymmetrical doublet with an intensity ratio of approximately 2:1 when their xylene-d_{10} solutions were heated to 130 °C (Figure 3a). The two-peak signal showed a large separation of approximately 111−66 Hz, too large for a geminal coupling between ester methylene protons, CH^{ε}_2 (Figure 3a).[69−71] Therefore, this peak intensity must be interpreted by assuming restricted rotation around the ester bond, $O-CH^{\varepsilon}_2$, through a three-site jump rotation generating three dynamic helical conformations called rotamers *A*, *B*, and *C* (Figures 4 and Figure S3).[49−51] Thereby, a so-called *M*-helix is assumed; in the case of a ***P***-helix, the three rotamers are depicted in Figure S3. The ratio of a relatively *contracted cis−cisoid* helix

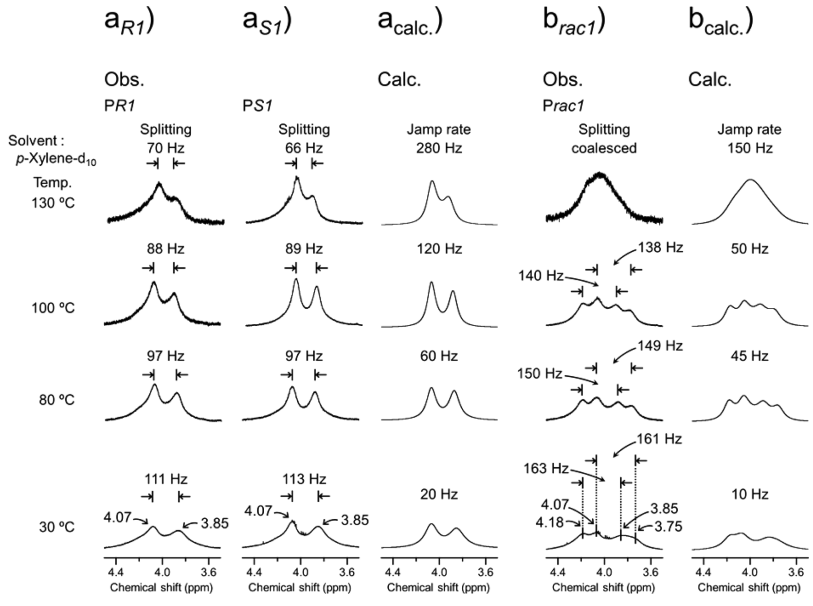

Figure 3. Temperature-dependent ^{1}H NMR spectra due to OCH^{ε}_2 protons observed at 30, 80, 100, and 130 °C and their simulated spectra expanded in the range 4.5−3.5 ppm.

DOI: 10.1021/acs.macromol.6b02508
Macromolecules XXXX, XXX, XXX−XXX

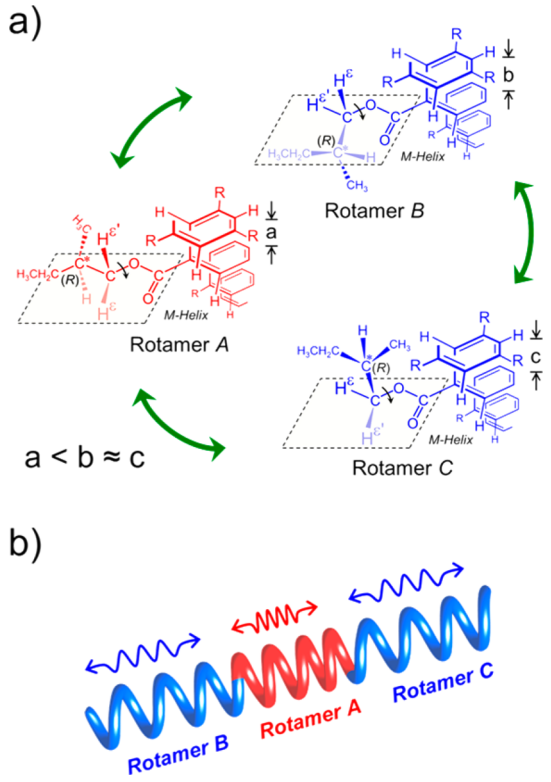

Figure 4. (a) Newman projection of rotamers *A*, *B*, and *C*. (b) An accordion-like helical oscillation (HELIOS) of **PR1** with *M*-helix composed of rotamers *A*, *B*, and *C*.

sequence due to rotamer *A* (red color) and slightly *stretched cis–cisoid* sequences comprising rotamers *B* and *C* (blue color) is approximately 1:2. This is similar to the case of poly(*n*-heptyl propiolate), **P*n*HepP**.[50] These rotamers undergo the so-called accordion-like helix oscillation (HELIOS) along the main chain axis within the time scale of the ^{1}H NMR experiment, i.e., 10^1–10^6 Hz.[72] The ester four-peak signal (intensity ratio, 2:2:1:1) of **Prac1** and **Pco** also showed a reversible, temperature-dependent change in line shape and intensity, where the four-peak signal ultimately becomes an extremely broad singlet (Figure 3b). Therefore, this change of **Prac1** must also be caused by restricted rotation around the racemic ester bond, as in the case of the chiral homopolymers. This difference in temperature also indicates that these polymers are thermally stable, as compared to **Ps2OcP** and **P*n*HepP**.[49−51] The observed four-peak signal must be attributed to magnetically different environments, i.e., the existence of two types of O−CH$^{e}_2$ moieties due to restricted rotation occurring in **Prac1**. The Gibbs free energy ($\Delta G^{\ddagger}$) of activation for rotation about the O−CH$^{e}_2$ bond was calculated from the observed temperature and the value of the peak splitting (Table. 3).[69−71,73,74] ^{1}H NMR spectral simulations of the two- and four-line signals were successfully accomplished using the gNMR program[67] to prove the chemical exchange assuming a three-site jump model without helix inversion (Figure 3). Furthermore, the kinetic data indicated that (i) the rotation of the O−CH$^{e}_2$ bond is restricted, (ii) the side chain of **Prac1** rotates much faster than that of the homochiral polymer, **PR1** or **PS1**, and (iii) the flexibility of **Prac1** is higher than that of **PR1** or **PS1**.

Determination of Proton Pairs Exchanging Their Magnetics Sites by 2D ROESY NMR Spectrum. The 2D ROESY spectrum of **Prac1** was measured to explicitly determine which peak combination for the four-peak signal belonged to the chemically exchanging protons (Figures 1a, 2a, and 3b). The relevant proton pairs were successfully detected as cross-peaks with a positive sign (green), when the diagonal peak was depicted as a positive sign (Figure 5). Thus, the four-peak signal was identified as a combination of the (a and c) peaks, and (b and d) peaks, respectively. The ROESY spectrum of **Prac1** also corroborated the assignment, since the exchangeable proton and the NOE proton have opposite signs with respect to the diagonal sign (Figures 5 and 6). The (a, d) protons and (b, c) protons were spatially close, within approximately 5 Å (Figure S4). Accordingly, in the helical main-chain of the *cis–cisoid* structure, the chirality of $n + 6$ and $n + 3$ monomer units was the same as and opposite to that of the n unit, respectively (Figure 6 and Figure S5). Therefore, the polymer with a one-handed helical sense main chain comprises an alternating sequence of ***R*1** and ***S*1** monomers (Figure 7). The four-peak signal, thus, points toward two diastereotopic relationships between the two helical senses (*P* and *M*) and the two chirality within the alkyl group ((*R*) and (*S*)). Moreover each peak is split into two peaks by the chemical exchange.

Table 3. Observed and Simulated Kinetic Dynamical Data for Restricted Rotation in the ^{1}H NMR Spectra of P*rac*1, PR1, and PS1[a]

	splitting (Hz)		jump rate (Hz)		
polymer	30 °C	130 °C	30 °C	130 °C	$\Delta G^{\ddagger}$ (kcal/mol)
Prac1	161, 163	–[b]	10	150	19.1
PR1	111	70	20	280	19.4
PS1	113	66	20	280	19.4

[a]Calculated by gNMR; peaks corresponding rotamer *A*, *B*, and *C* were calculated as equal populations. [b]Coalesced temperature.

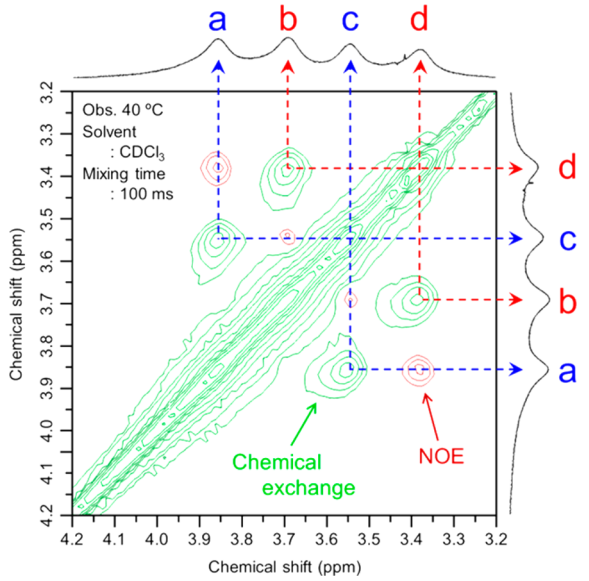

Figure 5. The 920 MHz ROESY NMR spectrum of **Prac1** expanded in the range of 4.2–3.2 ppm (40 °C in $CDCl_3$).

^{13}C NMR Spectra of P*rac*1, PR1, and PS1. The ^{13}C NMR spectrum of **Prac1** was measured (Figure 8a) to elucidate the monomer sequence of the resulting polymer chain. The two methyl signals due to the branched C$^{\eta\prime}$H$_3$ and the terminal CH$_3$ were split into asymmetric doublets whose peaks (16.8–

DOI: 10.1021/acs.macromol.6b02508
Macromolecules XXXX, XXX, XXX−XXX

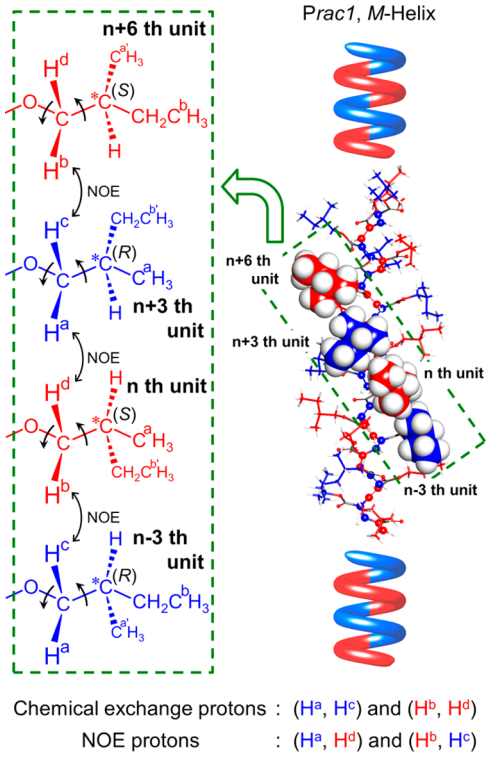

Figure 6. Side view of ***Prac*1** with *M*-helix showing spatial relations of $-OCH^{\varepsilon}{}_2-$ protons between the nearest-neighbor side chains, i.e., (a and c) proton pair and (b and d) proton pair between the *n*th unit and ($n \pm 3$)th unit, together with the ($n + 6$)th unit, in the helical main chain. The protons ($\mathbf{H}^{a}$ and $\mathbf{H}^{c}$) and ($\mathbf{H}^{b}$ and $\mathbf{H}^{d}$) are located on the ***R*1** unit and ***S*1** unit sides, respectively.

16.2 and 16.56−16.43, 11.4−11.0 and 11.20−11.10 ppm) are depicted in Figure 8b. However, in the case of **PR1** or **PS1**, the peaks due to $\mathbf{C}^{\eta'}\mathbf{H}_3$ at 16.6 ppm, the terminal CH_3 at 11.2 ppm (Figure S6), and the remaining signals of ***Prac*1**, **PR1**, and **PS1** were not split (Figure 8 and Figure S6).

Temperature Dependence of the Line Shapes of Two Methyl Carbons. The two split peaks due to the two methyl carbons of ***Prac*1** also showed a typical temperature-dependent shape (Figure 8b); the splitting width of each doublet decreased from 15.6 to 9.9 Hz in the $C^{\eta'}H_3$ and from 18.0 to 7.4 Hz in the terminal CH_3 when the temperature was increased from 0 to 60 °C. These spectral changes again point to restricted rotation around the $C^{\varepsilon}-{}^{*}C^{\zeta}$ bond in the alkyl side chain, although such restricted rotation was not observed for ***PR*1** or ***PS*1**. It should be noted that in the case of poly(*s*-2-octyl propiolate), ***Ps*2OctP**, such restricted rotation around the ester bond was clearly detected.[49] The restricted rotation models are depicted using a Newman projection as three conformers, $C_{(i)}$, $C_{(ii)}$, and $C_{(iii)}$, of the ***R*1** or ***S*1** moiety (Figure 8c and Figure S7). Among the three conformers, $C_{(ii)}$ has fairly large steric hindrance compared with $C_{(i)}$ or $C_{(iii)}$. Therefore, the lifetime of the $C_{(ii)}$ conformer among the three conformers is shorter than that of $C_{(i)}$ and $C_{(iii)}$ in the time scale of the ^{13}C NMR experiment. The relative weight among the three conformers due to branched $C^{\eta'}H_3$ is approximately $C_{(i)}:C_{(ii)}:C_{(iii)}$ = 1:0:1 at 60 °C (Figure 8b). On the other hand, the intensity ratio of the peak at 11.28 and 11.14 ppm due to the terminal CH_3 becomes approximately 2:1, indicating that the ratio of such conformers is $C_{(i)} + C_{(iii)}:C_{(ii)}$ = 2:1. This means that the intramolecular steric hindrance between the alkyl side chain in the racemic and chiral polymers is significantly different. This is understandable, as ***Prac*1** is composed of different chiral units, i.e., ***R*1** and ***S*1**, while the chiral polymers have a completely stereoregular microsequence (Figure 6 and Figure S5).

Monomer Feed Ratio Dependence of the Two Methyl Peaks Detected by ^{13}C NMR. The ^{13}C NMR spectral line shape of ***Pco*** gradually approached that of ***Prac*1** when the ratio of ***R*1** to ***S*1** was increased or decreased in the copolymer (Figure 9a). In contrast, the ^{13}C NMR spectrum of the blend polymer, ***Pble***, completely agreed with that of the homochiral polymers **PR1** or **PS1** (Figure 9a). The peak intensities at lower magnetic field due to $C^{\eta'}H_3$ and CH_3 increased with increasing monomer ratio of either ***R*1** or ***S*1** within the copolymer. Furthermore, the chemical shift of the increased peaks agreed with those of the chiral and blend polymers. This spectral change suggest that ***Pco*** is composed of only two sequences, i.e., homochiral and alternating sequences, and never includes a random sequence.

Calculation of Main Chain Dihedral Angles, Pitch Width, and Strain Energies. Dihedral angles between the two *cis* double bonds C=C−C=C in the helical main chain, the helical pitch width, and the strain energies of those helices[75] were calculated using the MMFF94 force field program for a 20-mer as a model of **PR1**, **PS1**, and ***Prac*1** (Figure 10 and

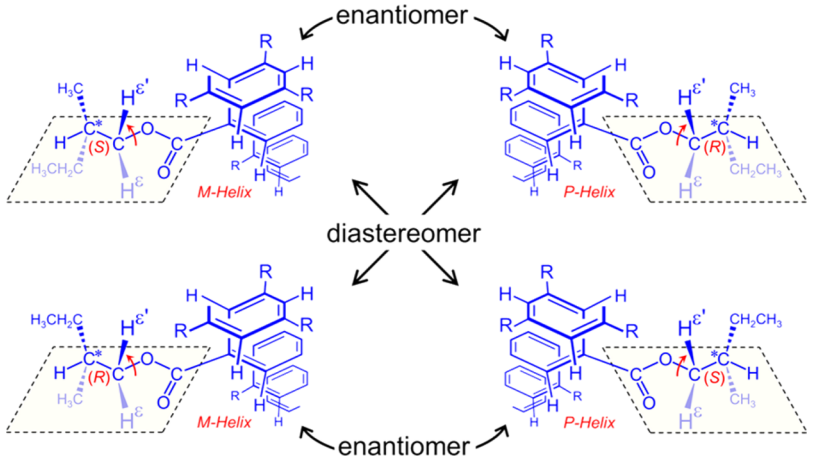

Figure 7. Perspective views of enantiomers and diastereomers with *P*- and *M*-helices in ***Prac*1**.

DOI: 10.1021/acs.macromol.6b02508
Macromolecules XXXX, XXX, XXX−XXX

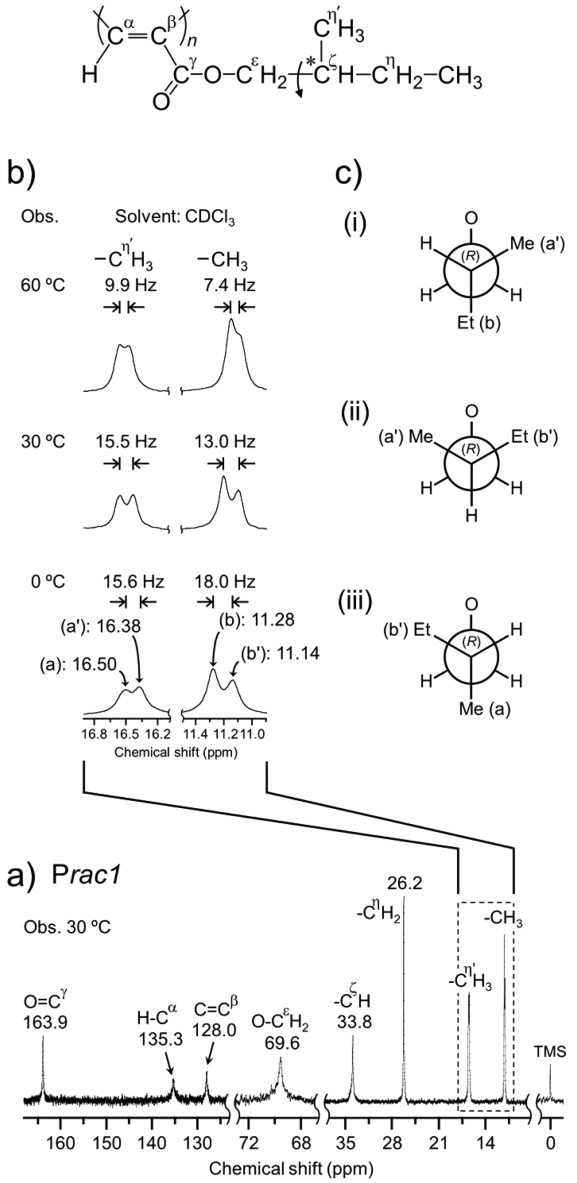

Figure 8. (a) ^{13}C NMR spectra of ***Prac*1** observed at 30 °C. (b) Temperature-dependent ^{13}C NMR spectra of branch $C^{\eta\prime}H_3$ and terminal CH_3 in ***Prac*1**. (c) The three-rotamer model depicted using a Newman projection for the side chain of **PR1**.

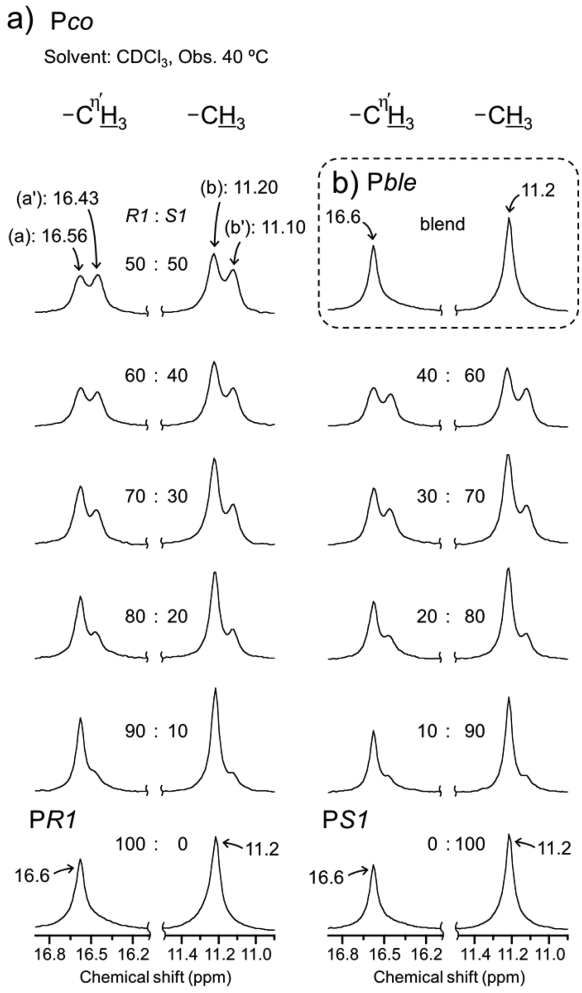

Figure 9. (a) Monomer feed dependence of ^{13}C NMR spectra due to branched $C^{\eta\prime}H_3$ and terminal CH_3 moieties in **Pco** and (b) ^{13}C NMR spectrum of ***Pble*** observed at 40 °C in $CDCl_3$. ***Pble*** was obtained by mixing **PR1** with **PS1** at a molar ratio of 50:50 in $CDCl_3$.

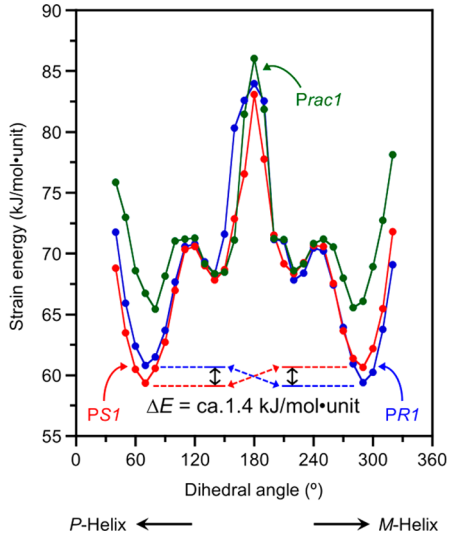

Figure 10. Calculated dihedral angles of C−C and C═C bonds, helical pitches, and strain energies of **PR1**, **PS1**, and ***Prac*1** using MMFF94.

Table 4).[66] The relevant helical sense polymers are depicted together with the relation between the diastereomer and the enantiomer in Figures 6 and 7 as well as Figure S5. The strain energy of **PR1** or **PS1** is smaller than that of ***Prac*1**, indicating that the conformation of ***Prac*1** is energetically unfavorable compared with that of **PR1** or **PS1**. These calculations also corroborate that each helical sense of **PR1** or **PS1** corresponds to that of the *M*-helix or *P*-helix, respectively, because the strain energies of each helical sense are larger than those of opposite senses, ΔE = ca. 1.4 kJ/mol at the dihedral angles, 70° and 290°. Furthermore, this indicates that the helical oscillated molecular chains of (**PR1** or **PS1**) and ***Prac*1** have small pitch widths (3.6 and 4.0 Å). The top and side views of *M*- and/or *P*-helix models in **PR1**, **PS1**, and ***Prac*1** are presented in Figure S8.

UV and CD Spectra of Contracted and Stretched Helices. The UV−vis spectra for **PR1**, **PS1**, and **Pco** exhibit

DOI: 10.1021/acs.macromol.6b02508
Macromolecules XXXX, XXX, XXX−XXX

Table 4. Helical Senses, Dihedral Angles of C−C and C═C Bonds, Helical Pitches, and Strain Energies of PR1, PS1, and P*rac*1 Using MMFF94[a]

polymer	helical sense	dihedral angle (deg)	pitch (Å)	strain energy[b] (kJ/(mol unit))
PR1	*M*-helix	290	3.6	59.4
	P-helix	70	3.6	60.8
PS1	*M*-helix	290	3.6	60.7
	P-helix	70	3.6	59.4
P*rac*1	*M*-helix	280	4.0	65.5
	P-helix	80	4.0	65.4

[a]Calculated by molecular mechanics method MMFF94. [b]Optimized structure of *P*-helix or *M*-helix.

two absorption maxima λ_{max} at 275 and 317 nm (Figure 11b) that are unaffected when the chiral monomer ratio ***R*1**:***S*1** is

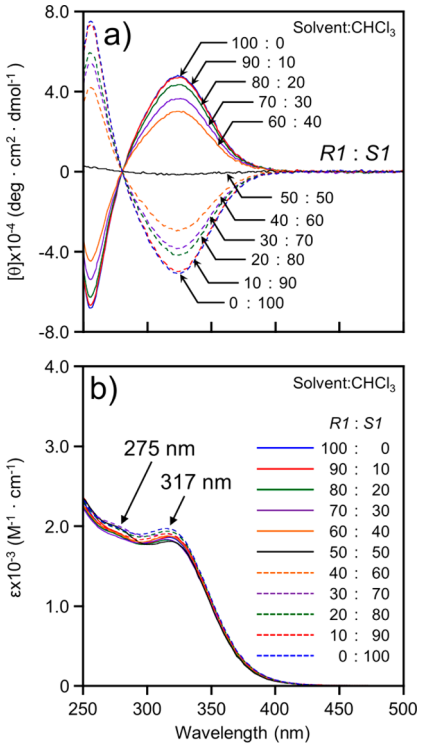

Figure 11. (a) Dependence of CD spectra of **PR1**, **PS1**, and **P*co*** on chiral monomer feed ($CHCl_3$ at 30 °C). (b) Dependence of UV−vis spectra of **PR1**, **PS1**, and **P*co*** on monomer feed ($CHCl_3$ at 30 °C).

changed from 100:0 to 0:100. This indicates that **PR1**, **PS1**, and **P*co*** are typical helical polymers having an accordion-like helix oscillation (HELIOS), as in the case for shrunk (= contracted) helices, such as **P*n*HepP**.[50] For comparison with the chiral polymers, **P*co*** and **P*n*HepP**, the two absorptions at 275 nm and 317 ppm can be attributed to the contracted *cis*−*cisoid* helix (rotamer *A*) and stretched *cis*−*cisoid* helices (= rotamers *B* and/or *C*) of **P*co*** and (**PR1** or **PS1**), respectively (Figure 4 and Figure S3).

The CD spectra of **P*co*s** and the chiral polymers **PR1** and **PS1** were also measured to determine the quantity of the predominant helical sense polymer by changing the feed ratio of the chiral monomer (Figure 11a). A Cotton effect at 325 nm in the CD spectra was observed, although the sign due to the helix of the main chain changed according to the chiral monomer ratio. Furthermore, when CD intensity at 317 nm was plotted as a function of the feed ratio of the chiral monomer (Figure 12b), there was no linear relation between

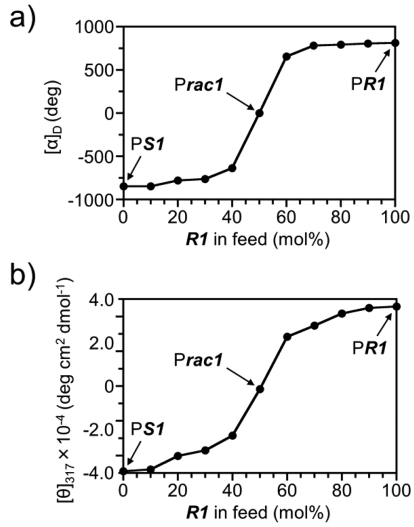

Figure 12. (a) Relationship between optical rotation and the feed ratio of ***R*1**. (b) CD spectral intensity dependence of ***R*1** monomer in the copolymer **P*co*** as observed at 317 nm in $CHCl_3$ at 30 °C.

optical rotation and the monomer feed ratio (Figures 11 and 12a). This suggests that the helix sense is biased by either the *M*- or *P*-helix, corresponding to the ***R*1** or ***S*1** monomers, respectively.

Polymerization Mechanism of Chiral *R*1 or *S*1 and Racemic *rac*1 Monomers. The monomeric rhodium complex as an important catalytic species is generated when methanol, with its electron lone pair, is used as the solvent (Scheme 1).[11−14] On the basis of the results shown above, we propose a polymerization mechanism to explain the observed alternating copolymer sequences. A unique copolymerization with alternating monomer sequence occurs when introducing five ***R*1** or ***S*1** monomers (Scheme 2). In the initiation step, the chiral monomer ***R*1** or ***S*1** coordinates to the monomeric Rh complex with the methanol molecule to generate the chiral Rh propagation chemical species. The resulting chiral Rh complex species selects ***R*1** or ***S*1** monomer to newly generate an important chiral Rh complex (CHIRHEX) catalyst. The resulting CHIRHEX catalyst coordinated with ***R*1** selects the ***S*1** monomer, and inversely, the chiral Rh complex coordinated with ***S*1** monomer selects the ***R*1** monomer. Thus, the chiral Rh complex consecutively induces copolymerization with alternating incorporation of monomers to create the polymer **P*rac*1**. In the case of **P*co***, the highly alternating copolymer under incorporation of the ***R*1** or ***S*1** monomer is produced until the less abundant monomer is completely consumed, at which point, highly stereoregular homopolymerization proceeds by incorporating the remaining monomers of ***R*1** or ***S*1** (Scheme 2b). Then the helical sense of **P*co*** is determined by the remaining excess chiral monomer sequence, although ***R*1** and ***S*1** monomers coordinate to the achiral monomeric Rh complex at the initial step of the copolymerization (Scheme 2 and Figure 13). Furthermore, the proposed mechanism rationalizes why the optical rotation depends on the monomer ratio (Figure 12a,b) and the helical sense excess also depend on the feed monomer ratio, e.g., ***R*1** monomer (Figure 13). Therefore, the

DOI: 10.1021/acs.macromol.6b02508
Macromolecules XXXX, XXX, XXX−XXX

Scheme 2. (a) Proposed Polymerization Mechanisms of *rac*1 To Generate the Alternative Copolymer; (b) Proposed Formation Mechanism of P*co* Using a Monomer Ratio of *R*1:*S*1 = 8:2

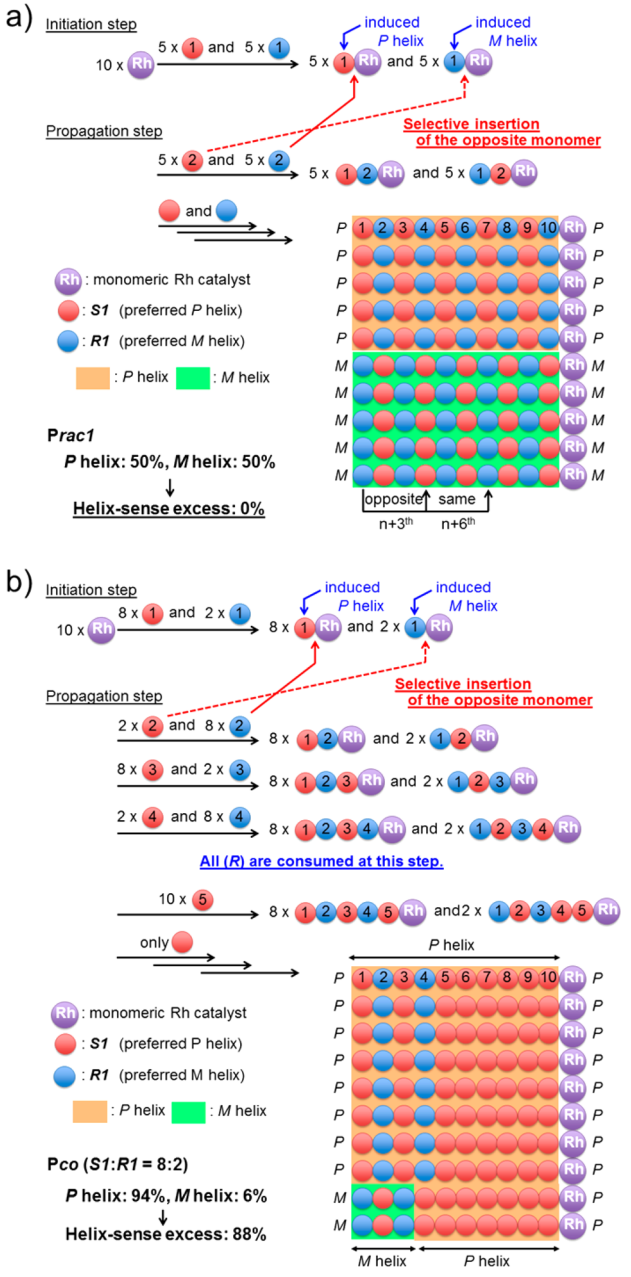

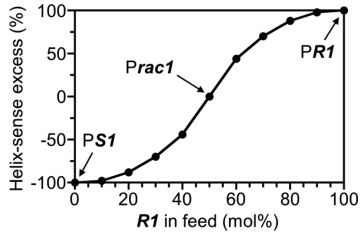

Figure 13. Helix sense excess (%) estimated using the feed ratio of ***R*1** monomer based on the Scheme 2.

copolymer possess both alternating and chiral homopolymer sequences. This feature can also explain why ***Prac*1** exhibits a four-peak signal, and ***PR*1** or ***PS*1** exhibit a two-peak signal in their ^{1}H NMR spectra. Thus, these results are reasonably explained even if the so-called dynamic helix inversion[55−59] is not accepted at present.

CONCLUSIONS

Monomers of DL-2-methyl-1-butyl propiolate (***rac*1**), (*R*)-2-methyl-1-butyl propiolate (***R*1**), and (*S*)-2-methyl-1-butyl propiolate (***S*1**) were stereoregularly polymerized using the catalyst [Rh(nbd)Cl]$_2$ at 40 °C in methanol to yield the corresponding racemic ***Prac*1** and chiral (***PR*1** and ***PS*1**) polymers. Temperature-dependent ^{1}H NMR spectra indicated restricted rotation around the ester O−CH$^{\varepsilon}_2$ bonds of the alkyl side chains. However, this phenomenon does not support the helix inversion model.[55−59] The asymmetric doublet peaks of the H$^{\varepsilon}$ proton (observed at 30−130 °C), with relative intensities of approximately 2:1, suggested three rotamers *A*, *B*, and *C*. The intensity ratio is in accord with a contracted *cis*−*cisoid* helix (*A*) and two relatively stretched *cis*−*cisoid* helices (*B* and *C*). The interesting four-peak signal observed in ***Prac*1** was interpreted in terms of a perfectly alternating copolymerization, i.e., *RSRSRS*, which was further corroborated by the 2D ROESY NMR spectrum. The ^{1}H NMR spectra and their simulation suggest that the alternating copolymer possesses a unique accordion-like helix oscillation (HELIOS) mode. Furthermore, the stable helical senses resulting from ***PR*1** and ***PS*1** were calculated by the MMFF94 program in their energetically favorable conformations. The two UV-absorption maxima observed at 275 and 317 nm also point to the formation of three helices. Based on these results, a polymerization mechanism was proposed to explain the formation of strictly stereoregular and alternating monomer sequences. The smallest helical pitch width, 3.6 Å, calculated in the two chiral polymers, is close to that of graphite, a typical conductive and layered material.[76−78] The present study is the starting point for further research into, for example, the fabrication of the smallest single helical polymer device, e.g., a sensitive magnetic nanosensor generating magnetic flux from the molecular axis to create an eternally oscillating nano molecular engine. These results are forthcoming.

ASSOCIATED CONTENT

Supporting Information

The Supporting Information is available free of charge on the ACS Publications website at DOI: 10.1021/acs.macromol.6b02508.

Figures S1−S8 (PDF)

AUTHOR INFORMATION

Corresponding Authors

*E-mail tabata@mmm.muroran-it.ac.jp (M.T.).
*E-mail mawatari@mmm.muroran-it.ac.jp (Y.M.).

ORCID

Klaus Müllen: 0000-0001-6630-8786
Masayoshi Tabata: 0000-0001-6650-9991

Notes

The authors declare no competing financial interest.

DOI: 10.1021/acs.macromol.6b02508
Macromolecules XXXX, XXX, XXX−XXX

■ ACKNOWLEDGMENTS

Thanks are extended to the Instrument Center at the Institute for Molecular Science for collecting the 920 MHz 2D NMR (NOESY and ROESY) and CD spectra measurements.

■ REFERENCES

(1) Okamoto, Y.; Ohta, K.; Yuki, H. Highly Asymmetric Selective Polymerization of (RS)-α-Methylbenzyl Methacrylate by Grignard Reagent-(−)-sparteine Catalyst Systems. *Chem. Lett.* **1977**, *6* (6), 617−620.

(2) Kamer, P. C. J.; Notle, R. J. M.; Drenth, W. Screw Sense Selective Polymerization of Achiral Isocyanides Catalyzed by Optically Active Nickel(II) Complexes. *J. Am. Chem. Soc.* **1988**, *110*, 6818−6825.

(3) Patten, T. E.; Novak, B. M. "Living" Titanium(IV) Catalyzed Coordination Polymerizations of Isocyanates. *J. Am. Chem. Soc.* **1991**, *113*, 5065−5066.

(4) Miller, R. D. Polysilane High Polymers. *Chem. Rev.* **1989**, *89*, 1359−1410.

(5) Deming, T. J.; Novak, B. M. Enantioselective Polymerizations of Achiral Isocyanides. Preparation of Optically Active Helical Polymers Using Chiral Nickel Catalysts. *J. Am. Chem. Soc.* **1992**, *114*, 7926−7927.

(6) Green, M. M.; Park, J.-W.; Sato, T.; Teramoto, A.; Lifson, S.; Selinger, R. L. B.; Selinger, J. V. The Macromolecular Route to Chiral Amplification. *Angew. Chem., Int. Ed.* **1999**, *38*, 3138−3154.

(7) Okamoto, Y.; Yashima, E. Asymmetric Polymerization of Methacrylates. *Prog. Polym. Sci.* **1990**, *15*, 263−298.

(8) Maeda, K.; Okamoto, Y. Synthesis and Conformation of Optically Active Poly(Aromatic Isocyanate)s. *Kobunshi Ronbunshu* **1997**, *54* (10), 608−620.

(9) Fujiki, M. Ideal Exciton Spectra in Single- and Double-Screw-Sense Helical Polysilanes. *J. Am. Chem. Soc.* **1994**, *116*, 6017−6018.

(10) Fujiki, M. Optically Active Polysilylenes: State-of-the-Art Chiroptical Polymers. *Macromol. Rapid Commun.* **2001**, *22*, 539−563.

(11) Tabata, M.; Yang, W.; Yokota, K. Polymerization of m-Chlorophenylacetylene Initiated by [Rh(norbornadiene)Cl]$_2$-Triethylamine Catalyst Containing Long-Lived Propagation Species. *Polym. J.* **1990**, *22*, 1105−1107.

(12) Yang, W.; Tabata, M.; Kobayashi, S.; Yokota, K.; Shimizu, A. Synthesis of Ultra-High-Molecular-Weight Aromatic Polyacetylenes with [Rh(norbornadiene)Cl]$_2$-Triethylamine and Solvent-Induced Crystallization of the Obtained Amorphous Polyacetylenes. *Polym. J.* **1991**, *23*, 1135−1138.

(13) Tabata, M.; Yang, W.; Yokota, K. ^{1}H-NMR and UV Studies of Rh Complexes as a Stereoregular Polymerization Catalysts for Phenylacetylenes: Effects of Ligands and Solvents on its Catalyst Activity. *J. Polym. Sci., Part A: Polym. Chem.* **1994**, *32*, 1113−1120.

(14) Lindgren, M.; Lee, H. S.; Yang, W.; Tabata, M.; Yokota, K. Synthesis of Soluble Polyphenylacetylenes Containing a Strong Donor Function. *Polymer* **1991**, *32*, 1531−1534.

(15) Tabata, M.; Kobayashi, S.; Sadahiro, Y.; Nozaki, Y.; Yokota, K.; Yang, W. Stereoregular Polymerization of Alkyl Propiolate Catalyzed by Rh Complex. *J. Macromol. Sci., Part A: Pure Appl.Chem.* **1994**, *31* (4), 465−475.

(16) Tabata, M.; Sadahiro, Y.; Sone, T.; Inaba, Y.; Yokota, K. Preparation of Polyacetylene Esters Bearing Pseudohexagonal Structures Using a Rh Complex Catalyst. *Kobunshi Ronbunshu* **1999**, *56* (6), 350−360.

(17) Nakako, H.; Nomura, R.; Tabata, M.; Masuda, T. Synthesis and Structure in Solution of Poly[(−)-menthyl propiolate] as a New Class of Helical Polyacetylene. *Macromolecules* **1999**, *32*, 2861−2864.

(18) Furlani, A.; Napoletano, C.; Russo, M. V.; Feast, W. J. Stereoregular polyphenylacetylene. *Polym. Bull.* **1986**, *16*, 311−317.

(19) Motoshige, R.; Mawatari, Y.; Motoshige, A.; Yoshida, Y.; Sasaki, T.; Yoshimizu, H.; Suzuki, T.; Tsujita, Y.; Tabata, M. Mutual Conversion between Stretched and Contracted Helices Accompanied by a Drastic Change in Color and Spatial Structure of Poly(phenylacetylene) Prepared with a [Rh(nbd)Cl]$_2$-Amine Catalyst. *J. Polym. Sci., Part A: Polym. Chem.* **2014**, *52*, 752−759.

(20) Tabata, M.; Kobayashi, S.; Sadahiro, Y.; Nozaki, Y.; Yokota, K.; Yang, W. Columnar Formation from Polyethynylbenzene and Poly-(p-Methylethynylbenzene) Polymerized Using [Rh(norbornadiene)Cl]$_2$ as a Catalyst. An X-ray and ESR Study. *J. Macromol. Sci., Part A: Pure Appl.Chem.* **1997**, *34* (4), 641−653.

(21) Sato, E.; Mawatari, Y.; Sadahiro, Y.; Yamada, B.; Tabata, M.; Kashiwaya, Y. Geometrical structures of poly(haloalkyl propiolate)s prepared with a [Rh(norbornadiene)Cl]$_2$ catalyst. *Polymer* **2008**, *49*, 1620−1628.

(22) Mawatari, Y.; Tabata, M. Color Changes Caused by Structures of Stereoregular Substituted-Polyacetylenes. *Shikizai Kyokaishi* **2009**, *82*, 204−209.

(23) Motoshige, A.; Mawatari, Y.; Yoshida, Y.; Seki, C.; Matsuyama, H.; Tabata, M. Irreversible Helix Rearrangement from Cis-Transoid to Cis-Cisoid in Poly(p-n-hexyloxyphenylacetylene) Induced by Heat-Treatment in Solid Phase. *J. Polym. Sci., Part A: Polym. Chem.* **2012**, *50*, 3008−3015.

(24) Motoshige, A.; Mawatari, Y.; Motoshige, R.; Yoshida, Y.; Tabata, M. *J. Polym. Sci., Part A: Polym. Chem.* **2013**, *51*, 5177−5183.

(25) Motoshige, A.; Mawatari, Y.; Motoshige, R.; Yoshida, Y.; Tabata, M. Synthesis and Solid State Helix to Helix Rearrangement of Poly(phenylacetylene) bearing n-Octyl Alkyl Aide Ahains. *Polym. Chem.* **2014**, *5*, 971−978.

(26) Mawatari, Y.; Yoshida, Y.; Motoshige, A.; Motoshige, R.; Sasaki, T.; Tabata, M. Solid Phase Helical and Crystal Structures of Poly(phenylacetylene)s with Para-oligo Ethylene Oxymethylether Moieties Prepared with an Organorhodium Catalyst in Ethanol. *Eur. Polym. J.* **2014**, *57*, 213−220.

(27) Sasaki, T.; Yoshida, Y.; Mawatari, Y.; Tabata, M. Remarkably Stretched Cis-Transoid Helices Generated in Solid Phase and Solution of Poly(carbazole acetylene) Prepared Using an Organorhodium Catalyst in Toluene. *Macromolecules* **2015**, *48*, 889−897.

(28) Masuda, T.; Abdul Karim, S. M.; Nomura, R. Synthesis of Acetylene-Based Widely Conjugated Polymers by Metathesis Polymerization and Polymer Properties. *J. Mol. Catal. A: Chem.* **2000**, *160* (1), 125−131.

(29) Nomura, R.; Nakako, H.; Masuda, T. Design and Synthesis of Semiflexible Substituted Polyacetylenes with Helical Conformation. *J. Mol. Catal. A: Chem.* **2002**, *190*, 197−205.

(30) Maeda, K.; Yashima, E. Helicity Induction on Macromolecules. *Yuki Gosei Kagaku Kyokaishi* **2002**, *60*, 878−890.

(31) Hadano, S.; Kishimoto, T.; Hattori, T.; Tanioka, D.; Teraguchi, M.; Aoki, T.; Kaneko, T.; Namikoshi, T.; Marwanta, E. Helix-Sense-Selective Polymerization of Achiral Bis(hydroxymethyl)-phenylacetylenes Bearing Alkyl Groups of Different Lengths. *Macromol. Chem. Phys.* **2009**, *210*, 717−727.

(32) Liu, L.; Mottate, K.; Zhang, G.; Aoki, T.; Kaneko, T.; Teraguchi, M. Chiral Amplification during Asymmetric-Induced Copolymerization of Phenylacetylenes with Tight Cis-Cisoidal Main Chains. *Macromol. Rapid Commun.* **2013**, *34*, 1140−1144.

(33) Nakazono, K.; Fukasawa, K.; Sato, T.; Koyama, Y.; Takata, T. Synthesis of Acetylene-Functionalized [2]Rotaxane Monomers Directed toward Side Chain-Type Polyrotaxanes. *Polym. J.* **2010**, *42*, 208−215.

(34) Masuda, T. Substituted Polyacetylenes. *J. Polym. Sci., Part A: Polym. Chem.* **2007**, *45*, 165−180.

(35) Yashima, E.; Maeda, K.; Iida, H.; Furusho, Y.; Nagai, K. Helical Polymers: Synthesis, Structures, and Functions. *Chem. Rev.* **2009**, *109*, 6102−6211.

(36) Aoki, T.; Kaneko, T.; Teraguchi, M. Synthesis of Functional π-Conjugated Polymers from Aromatic Acetylenes. *Polymer* **2006**, *47*, 4867−4892.

(37) Liu, J.; Lam, J. W. Y.; Tang, B. Z. Acetylenic Polymers: Syntheses, Structures, and Functions. *Chem. Rev.* **2009**, *109*, 5799−5867.

DOI: 10.1021/acs.macromol.6b02508
Macromolecules XXXX, XXX, XXX−XXX

(38) Zhang, W.; Tabei, J.; Shiotsuki, M.; Masuda, T. Synthesis of Poly(propargyl esters) with Rhodium Catalysts and Their Characterization. *Polym. Bull.* **2006**, *57*, 463−472.
(39) Suzuki, Y.; Shiotsuki, M.; Sanda, F.; Masuda, T. Chiral 1-Methylpropargyl Alcohol: A Simple and Powerful Helical Source for Substituted Polyacetylenes. *Macromolecules* **2007**, *40*, 1864−1867.
(40) Suzuki, Y.; Shiotsuki, M.; Sanda, F.; Masuda, T. Synthesis and Helical Structure of Poly(1-methylpropargyl ester)s with Various Side Chains. *Chem. - Asian J.* **2008**, *3*, 2075−2081.
(41) Yoshida, Y.; Mawatari, Y.; Seki, C.; Hiraoki, T.; Matsuyama, H.; Tabata, M. Cis and Trans Radicals Generated in Helical Poly(propargyl acetate)s Prepared using a $[Rh(norbornadiene)Cl]_2$ Catalyst. *Polymer* **2011**, *52*, 646−651.
(42) Yoshida, Y.; Mawatari, Y.; Seki, C.; Hiraoki, T.; Matsuyama, H.; Tabata, M. Geometrical Structures in Solution and Solid Phase of Poly(propargyl ester)s Prepared by using a $[Rh(norbornadiene)Cl]_2$-Cocatalyst. *Polymer* **2011**, *52*, 3917−3924.
(43) Sanda, F.; Masuda, T. Synthesis and Functions of Optically Active Helical Conjugated Polymers. *Yuki Gosei Kagaku Kyokaishi* **2008**, *66*, 757−764.
(44) Nomura, R.; Tabei, J.; Masuda, T. Effect of Side Chain Structure on the Conformation of Poly(*N*-propargylalkylamide). *Macromolecules* **2002**, *35*, 2955−2961.
(45) Suenaga, M.; Kaneko, Y.; Kadokawa, J.; Nishikawa, T.; Mori, H.; Tabata, M. Amphiphilic Poly(*N*-propargylamide) with Galactose and Lauryloyl Groups: Synthesis and Properties. *Macromol. Biosci.* **2006**, *6*, 1009−1018.
(46) Minakawa, H.; Tabata, M.; Yokota, K. Structural Differences between Polypentynoates Bearing Mesogenic Moieties Polymerized with RH Complex and WCl_6 Catalysts. A ^{13}C-NMR and Raman Study. *J. Macromol. Sci., Part A: Pure Appl.Chem.* **1996**, *33* (3), 291−303.
(47) Tabata, M.; Namioka, M.; Yokota, K.; Minakawa, H. Structural Differences of Poly(α-ethynylnaphthalene)s obtained with $[Rh(norbornadiene)Cl]_2$ and WCl_6 Catalysts: An Electron Spin Resonance and Raman Study. *Polymer* **1996**, *37*, 1959−1963.
(48) Mawatari, Y.; Motoshige, A.; Yoshida, Y.; Motoshige, R.; Sasaki, T.; Tabata, M. Structural Determination of Stretched Helix and Contracted Helix Having Yellow and Red Colors of Poly(2-ethynylnaphthalene) Prepared with a $[Rh(norbornadiene)Cl]_2$-triethylamine Catalyst. *Polymer* **2014**, *55*, 2356−2361.
(49) Yoshida, Y.; Mawatari, Y.; Motoshige, A.; Motoshige, R.; Hiraoki, T.; Wagner, M.; Müllen, K.; Tabata, M. Accordion-like Oscillation of Contracted and Stretched Helices of Polyacetylenes Synchronized with the Restricted Rotation of Side Chains. *J. Am. Chem. Soc.* **2013**, *135*, 4110−4116.
(50) Yoshida, Y.; Mawatari, Y.; Motoshige, A.; Motodshige, R.; Hiraoki, T.; Tabata, M. Helix Oscillation of Polyacetylene Esters Detected by Dynamic ^1H NMR, IR, and UV-vis Methods in Solution. *Polym. Chem.* **2013**, *4*, 2982−2988.
(51) Yoshida, Y.; Mawatari, Y.; Tabata, M. Synthesis and Helix Pitch Control of π-Conjugated Helical Polymers with Accordion-like Oscillation. *Yuki Gosei Kagaku Kyokaishi* **2014**, *72*, 292−301.
(52) Tabata, M.; Sadahiro, Y.; Nozaki, Y.; Inaba, Y.; Yokota, K. Hexagonal Columns of Poly(*n*-alkyl propiolate) Produced with Rhodium Complex Catalyst. X-ray Analysis and Oxygen Permeability. *Macromolecules* **1996**, *29*, 6673−6675.
(53) Kozuka, M.; Sone, T.; Tabata, M.; Sadahiro, Y.; Enoto, T. Radiation-induced Cis to Trans Isomerization of Poly(*n*-butylpropiolate) Prepared with a $[Rh(norbornadiene)Cl]_2$ Complex as a Stereospecific Catalyst. *Radiat. Phys. Chem.* **2002**, *63*, 59−61.
(54) Kozuka, M.; Sone, T.; Sadahiro, Y.; Tabata, M.; Enoto, T. Columnar Assemblies of Aliphatic Poly(acetylene ester)s Prepared with a $[Rh(norbornadiene)Cl]_2$ Catalyst. ^1H and ^{13}C NMR, X-Ray Diffraction and AFM Studies. *Macromol. Chem. Phys.* **2002**, *203*, 66−70.
(55) Nomura, R.; Fukushima, Y.; Nakako, H.; Masuda, T. Conformational Study of Helical Poly(propiolic esters) in Solution. *J. Am. Chem. Soc.* **2000**, *122*, 8830−8836.
(56) Nakako, H.; Mayahara, Y.; Nomura, R.; Tabata, M.; Masuda, T. Effect of Chiral Substituents on the Helical Conformation of Poly(propiolic esters). *Macromolecules* **2000**, *33*, 3978−3982.
(57) Nakako, H.; Nomura, R.; Masuda, T. Helix Inversion of Poly(propiolic esters). *Macromolecules* **2001**, *34*, 1496−1502.
(58) Ishiwari, F.; Fukasawa, K.; Sato, T.; Nakazono, K.; Koyama, Y.; Takata, T. A Rational Design for the Directed Helicity Change of Polyacetylene Using Dynamic Rotaxane Mobility by Means of Through-Space Chirality Transfer. *Chem. - Eur. J.* **2011**, *17*, 12067−12075.
(59) Freire, F.; Seco, J. M.; Quiñoá, E.; Riguera, R. Nanospheres with Tunable Size and Chirality from Helical Polymer-Metal Complexes. *J. Am. Chem. Soc.* **2012**, *134*, 19374−19383.
(60) Cowie, J. M. G., Ed.; *Alternating Copolymers*; Plenum Press: New York, 1985.
(61) Bataille, P.; Granger, F. Mechanical and Thermal Properties of an Alternating Methyl Methacrylate Styrene Copolymer. *Polym. Eng. Sci.* **1985**, *25*, 1164−1170.
(62) Rinaldi, P. L.; Hensley, D. R.; Tokles, M.; Hatvany, G. S.; Harwood, H. J. Application of {Deuterium}Carbon-13 INEPT NMR to the Study of Polymer Reactivity. *Macromolecules* **1992**, *25* (26), 7398−7399.
(63) Lutz, J.-F.; Kirci, B.; Matyjaszewski, K. Synthesis of Well-Defined Alternating Copolymers by Controlled/Living Radical Polymerization in the Presence of Lewis Acids. *Macromolecules* **2003**, *36*, 3136−3145.
(64) Yoshida, Y.; Endo, T. Synthesis and Thermal Properties of Vinyl Copolymers with Phenyl Vinylethylene Carbonate and *N*-Substituted Maleimides undergoing Color Change with Acid−Base Switching. *Polym. Chem.* **2016**, *7*, 6770−6778.
(65) Gawley, R. E. Do the Terms "% ee" and "% de" Make Sense as Expressions of Stereoisomer Composition or Stereoselectivity? *J. Org. Chem.* **2006**, *71*, 2411−2416.
(66) Halgren, T. A. Merck Molecular Force Field. I. Basis, Form, Scope, Parameterization, and Performance of MMFF94. *J. Comput. Chem.* **1996**, *17*, 490−519.
(67) The simulations of NMR spectra were carried out with a gNMR program, ver. 5.0, Ivory Soft.
(68) Tai, A.; Syouno, E.; Tanaka, K.; Fujita, M.; Sugimura, T.; Higashiura, Y.; Kakizaki, M.; Hara, H.; Naito, T. Regio- and Stereochemical Study of Sex Pheromone of Pine Sawfly. *Bull. Chem. Soc. Jpn.* **2002**, *75*, 111−121.
(69) Fraenkel, G.; Franconi, C. Protonation of Amides. *J. Am. Chem. Soc.* **1960**, *82*, 4478−4483.
(70) Woodbrey, J. C.; Rogers, M. T. Solvent Effects on the Energy Barrier for Hindered Internal Rotation in Some *N,N*-Disubstituted Amides. *J. Am. Chem. Soc.* **1962**, *84*, 13−16.
(71) Gehring, D. G.; Mosher, W. A.; Reddy, G. S. A Study of Hindered Internal Rotation in Some *N*-Vinyl-Substituted Amides by Nuclear Magnetic Resonance Spectroscopy. *J. Org. Chem.* **1966**, *31*, 3436−3437.
(72) Bryant, R. G. The NMR time scale. *J. Chem. Educ.* **1983**, *60*, 933−935.
(73) LaPlanche, L. A.; Rogers, M. T. Configurations in Unsymmetrically *N,N*-Disubstituted Amides. *J. Am. Chem. Soc.* **1963**, *85*, 3728−3730.
(74) Neuman, R. C.; Roark, D. N.; Jonas, V. Studies of Chemical Exchange by Nuclear Magnetic Resonance. II. Hindered Rotation in Amides and Thioamides. *J. Am. Chem. Soc.* **1967**, *89*, 3412−3416.
(75) Moss, G. P. Basic Terminology of Stereochemistry. *Pure Appl. Chem.* **1996**, *68*, 2193−2222.
(76) Delhaès, P., Ed.; *Graphite and Precursor*; Gordon and Breach: Amsterdam, 2001.
(77) Novoselov, K. S.; Geim, A. K.; Morozov, S. V.; Jiang, D.; Zhang, Y.; Dubonos, S. V.; et al. Electric Field Effect in Atomically Thin Carbon Films. *Science* **2004**, *306*, 666−669.
(78) Pisula, W.; Feng, X.; Müllen, K. Charge-Carrier Transporting Graphene-Type Molecules. *Chem. Mater.* **2011**, *23*, 554−567.

DOI: 10.1021/acs.macromol.6b02508
Macromolecules XXXX, XXX, XXX−XXX